Scanning tunneling microscopy/spectroscopy of picene thin films formed on Ag(111)

Yasuo Yoshida,[1,a)] Hung-Hsiang Yang,[2] Hsu-Sheng Huang,[3] Shu-You Guan,[3] Susumu Yanagisawa,[4] Takuya Yokosuka,[1] Minn-Tsong Lin,[2,5] Wei-Bin Su,[3] Chia-Seng Chang,[3] Germar Hoffmann,[1,6] and Yukio Hasegawa[1,b)]
[1]*The Institute of Solid State Physics, The University of Tokyo, Kashiwa 277-8581, Japan*
[2]*Department of Physics, National Taiwan University, Taipei 106, Taiwan*
[3]*Institute of Physics, Academia Sinica, Nankang, Taipei 11529, Taiwan*
[4]*Department of Physics and Earth Science Department, University of the Ryukyus, 1 Nishihara, Okinawa 903-0213, Japan*
[5]*Institute of Atomic and Molecular Sciences, Academia Sinica, Taipei 10617, Taiwan*
[6]*Department of Physics, National Tsing Hua University, Hsinchu 30013, Taiwan*

(Received 13 June 2014; accepted 15 August 2014; published online 16 September 2014)

Using ultrahigh-vacuum low-temperature scanning tunneling microscopy and spectroscopy combined with first principles density functional theory calculations, we have investigated structural and electronic properties of pristine and potassium (K)-deposited picene thin films formed *in situ* on a Ag(111) substrate. At low coverages, the molecules are uniformly distributed with the long axis aligned along the $[11\bar{2}]$ direction of the substrate. At higher coverages, ordered structures composed of monolayer molecules are observed, one of which is a monolayer with tilted and flat-lying molecules resembling a $(1\bar{1}0)$ plane of the bulk crystalline picene. Between the molecules and the substrate, the van der Waals interaction is dominant with negligible hybridization between their electronic states; a conclusion that contrasts with the chemisorption exhibited by pentacene molecules on the same substrate. We also observed a monolayer picene thin film in which all molecules were standing to form an intermolecular π stacking. Two-dimensional delocalized electronic states are found on the K-deposited π stacking structure. © *2014 AIP Publishing LLC*. [http://dx.doi.org/10.1063/1.4894439]

I. INTRODUCTION

Picene ($C_{22}H_{14}$), its chemical structure depicted in Fig. 1(c), is a simple aromatic compound composed of five fused benzene rings with an arm-chair edge. Thin films of one of its isomers, pentacene, possessing instead a zigzag edge, have been studied extensively because their high carrier mobility makes them a promising candidate for molecular electronic device applications such as organic field effect transistors[1–3] and photovoltaic cells.[4,5] However, instability or degradation of the molecule under atmospheric conditions remains a fundamental limitation to the pursuit of these practical applications.[6] Picene is chemically stable due to the large energy band gap (3.3 eV), compared with pentacene (1.8 eV), but has delocalized π-electrons in thin films and high carrier mobility under oxygen exposure,[6] a combination of the properties making it a promising post-pentacene candidate material for molecular electronics. Very recently, the molecule has attracted tremendous attention for an entirely different property, namely, the discovery of superconductivity in potassium (K)-doped picene with the critical temperature of 19 K,[7] followed by discoveries of similar aromatic compound-based superconductors with even higher transition temperatures up to 30 K.[8,9] In spite of this surprisingly high transition temperature, high reactivity in the air limits experimental access to K-doped picene, and therefore, molecular level details of growth, structural, and electronic properties have remained elusive.

The properties of the molecular thin films depend on the nature of the interfaces between the molecules and the substrate.[10] Understanding the contacts is a major motivation behind a study of molecular layer formation on surfaces. The performance of molecular devices also depends on the relative alignment of energy levels in the molecules, which may be strongly modified by the interaction of substrate electronic states with molecular orbitals.[11] Here, in order to understand structural and electronic properties of the molecular layer and their interactions with the substrate, we investigated ultrathin films of picene formed on a Ag(111) substrate *in situ* under ultrahigh vacuum (UHV) conditions by low-temperature scanning tunneling microscopy and spectroscopy (STM/STS) combined with first principles density functional theory (DFT) calculations. The obtained results indicate that the molecule has a weak van der Waals (vdW) interaction with the substrate (in contrast with pentacene on Ag(111)), and thus exhibits a growth mode different from that of the sister molecule.

II. METHODS

A. STM experiment

The experiments were performed using an ultrahigh vacuum STM setup (USM-1300, Unisoku, and SPM-1000, RHK)

a)E-mail: yyoshida@issp.u-tokyo.ac.jp
b)Author to whom correspondence should be addressed. Electronic mail: hasegawa@issp.u-tokyo.ac.jp

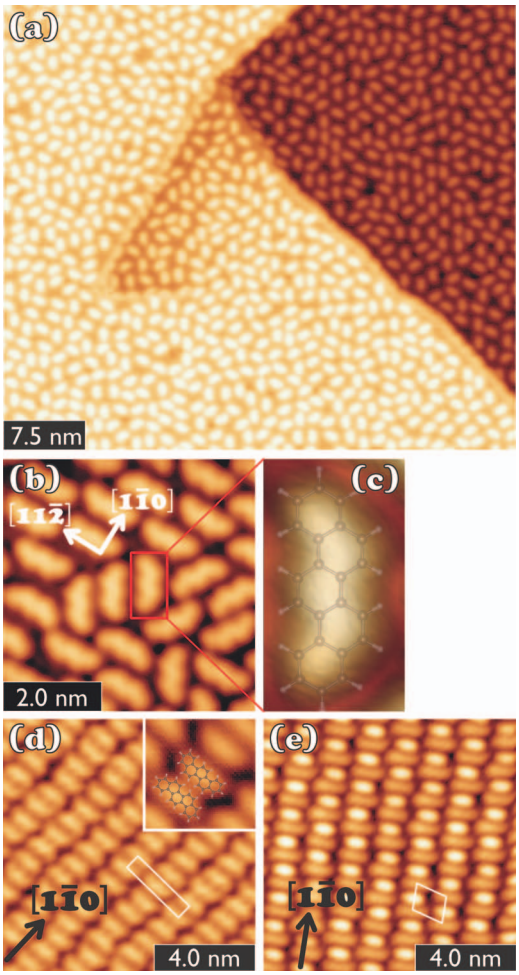

FIG. 1. (a) and (b) STM images of 0.7 ML picene-deposited Ag(111) surface. The sample bias voltage (V_s) and the tunneling current (I_t) are 1.0 V and 96 pA for (a) and 1.0 V and 290 pA for (b), respectively. (c) Zoomed image superimposed with a chemical formula of a picene molecule. (d) and (e) STM images of various monolayer picene thin film structures that we call phase 1 and phase 2, respectively, throughout this paper. The amount of deposited picene molecule is 1.0–1.5 ML. $V_s = 1.0$ V and $I_t = 48$ pA for (c), and $V_s = 1.0$ V and $I_t = 290$ pA for (d).

in which the tip and sample can be cooled down to ∼2.6 K at the Institute for Solid State Physics, the University of Tokyo. First, a single crystalline Ag(111) substrate was cleaned by repetitive Ar sputtering and annealing at ∼800 °C. After checking the cleanness and flatness of the surface by STM observation, picene molecules (99.9%, Nard Institute Ltd.) were deposited on the substrate using an evaporator heated around 100 °C. The amount of deposited molecules was estimated from low-coverage STM images, such as the ones shown in Figs. 1(a) and 1(b), assuming all deposited molecules adsorb on the substrate. The deposition/adsorption rate is 1.8×10^{-4} molecules/s nm^2. If we define 1 monolayer (ML) of picene thin film as a flat-lying structure whose molecular density is 0.95 molecule/nm^2 shown in Fig. 1(d), the deposition rate corresponds to 1.9×10^{-4} ML/s. The amount of deposited molecules was controlled by adjusting the deposition time. Potassium was deposited by heating a dispenser (SAES Getters). During both depositions, the substrate was kept at room temperature, and after the *in situ* deposition, the sample was transferred to the STM setup for characterization.

All the STM/STS measurements were performed at 4.2 K. Electrochemically etched W tips, which were annealed at ∼900 °C *in situ* for removing the oxide layer from the tip apex, were used for the imaging and spectroscopic measurements. The differential tunneling conductance spectra were taken using a standard lock-in method with a modulation of 50 mV_{rms} and 9.2 kHz on the sample bias voltage.

B. DFT calculation

For the first-principles DFT calculations, periodic slab models were employed to simulate a Ag(111) surface. We used a three atomic fcc layer Ag(111) slab with the optimized lattice constant of 0.408 nm, in close agreement with the experimental value (0.409 nm).[12] Vacuum regions equivalent to 12 atomic layers (∼2.8 nm) were inserted between the Ag slabs. For the DFT calculations, the STATE program code[13] was used, which employs pseudo-potentials to describe electron ion interactions.[14,15] Nonlinear core correction was included. The valence states were expanded by a plane wave basis set. The surface Brillouin zone was sampled by 1×2 and 2×2 **k**-point meshes for the phase 1 and phase 2 calculations, respectively. We used energy cutoffs of 25 Ry and 225 Ry for wave functions and augmented charge densities, respectively. The Fermi level was treated with the first-order Hermite-Gaussian scheme with the width of 0.05 eV.[16] To describe the vdW interaction between the adsorbate and the substrate, and among the adsorbates, we employed the gradient-corrected Perdew-Burke-Ernzerhof (PBE)[17] exchange-correlation potential including the semi-empirical dispersion correction proposed by Grimme,[18] which we call PBE-D. The atomic geometries of the adsorbed molecules and the upper two atomic layers of the Ag(111) slab were allowed to relax until the forces on all the atoms were below 0.08 nN. From the calculated atomic and electronic structures STM images were simulated with a scheme of the Tersoff-Hamann theory[19] by making a contour map of local density of states (LDOS) at 2.5×10^{-6} bohr^{-3} within an energy range between the Fermi level and the one corresponding to the set bias voltage.

III. RESULTS AND DISCUSSION

A. Low coverage adsorption of picene molecules

After the deposition of a small amount (∼0.7 ML) of picene molecules on the Ag(111) surface, we obtained STM images shown in Figs. 1(a) and 1(b). Zigzag-shaped individual picene molecules are clearly observed. The shape indicates that the adsorbed molecules lay their flat plane parallel to the substrate surface. The area density is 0.69 molecules/nm^2. In the images, the molecules are uniformly distributed over the substrate with an almost equal spacing between their nearest neighbors. The uniform distribution implies a repulsive interaction between them, which is obviously mediated through the substrate[20–22] because of their large separation. In the molecule, because of the different electron affinities, hydrogen (carbon) atoms are positively (negatively) charged. Therefore, on the substrate below hydrogen atoms electrons are collected whereas below carbon atoms holes are

collected. Since the edge of molecules is completely occupied by hydrogen atoms, the electron clouds below the molecules repel each other and contribute to the repulsive interaction among the adsorbed molecules. No bright protrusions are found at the ends of the molecules, indicating no bending, unlike the case of pentacene molecules deposited on Cu(111).[23] All picene molecules align their long axis along the [11$\bar{2}$] direction of the substrate. The orientation is also different from that of pentacene molecules adsorbed on Cu(111)[23] and Ag(111),[24] where the long axis of the adsorbed molecules align to the close-packed [1$\bar{1}$0] directions.

B. Monolayer coverage structures of picene molecules

Further molecular deposition (1.0–1.5 ML) makes various ordered structures of the adsorbed molecules, as shown in Figs. 1(d) and 1(e), and 6(a) in a sequence of the molecular density. In the lowest-density structure shown in Fig. 1(d), which we call phase 1 hereafter, the molecules make rows along the [1$\bar{1}$0] direction of the Ag substrate with their long axis aligned to the [11$\bar{2}$] direction. Judging from the observed bright protrusions similar in size to that of the isolated molecules, as demonstrated with a superimposed structural formula in an inset of Fig. 1(d), the molecules are most likely laid flat parallel to the substrate surface. Despite random orientations of the zigzag shape of the molecule, translational periodicities of the center of the molecules are obvious in the row and inter-row directions. The two-dimensionally (2D) ordered molecular structure has a centered rectangular unit cell, depicted with a white box in Fig. 1(d), with a space group of cm whose lengths are 0.75 ± 0.05 nm and 2.8 ± 0.2 nm. The density of the molecule is 0.95 ± 0.06 molecules/nm^2. The unit length along the close-packed direction is ∼2.5 times the Ag(111) atomic distance (0.298 nm); 2 intermolecular spacings correspond to 5 atom spacings of the substrate. The structure is symmetric with respect to the (1$\bar{1}$0) and ($\bar{1}\bar{1}$2) planes of the substrate except for the randomness of the zigzag orientation and slight meanderings of the molecular rows.

Whereas all molecules are laid flat in phase 1, the structure shown in Fig. 1(e) – phase 2 – has two kinds of protrusions, bright and dark, in the unit cell. The bright protrusion in the structure has a narrow shape implying it is a tilted molecule while the dark one looks flatter. The STM image of Fig. 2(b) shows a boundary between phase 1 and phase 2 and their structural relations. It is found that phase 2 has molecular rows along the [1$\bar{1}$0] direction, and the spacing between the neighboring rows is the same as in phase 1. As shown in Fig. 2(a), the height difference between the flat molecules in phase 1 and bright (dark) protrusions is only 0.25 nm (0.2 nm). These are much shorter than the short axis of the molecule (0.55 nm), thus phase 2 cannot be a layer formed over phase 1 even by considering possible modification in apparent height due to the electronic effect, which might happen in STM imaging. It is, therefore, natural to conclude that phase 2 is a monolayer directly formed on the substrate in which tilted and flat-lying molecules are alternatively arranged along the [1$\bar{1}$0] direction. The molecular rows of phase 2 are straight compared with those in phase 1, and the translational ordering is obviously improved. The mirror symmetry with respect to the (1$\bar{1}$0) plane is, however, broken. In fact, we observed all six domains over the sample whose unit cell is along the three equivalent [1$\bar{1}$0] directions with two orientations that have a mirror-reflected relation with respect to the (1$\bar{1}$0) plain, although the two orientations are not exactly equivalent on the Ag(111) substrate.

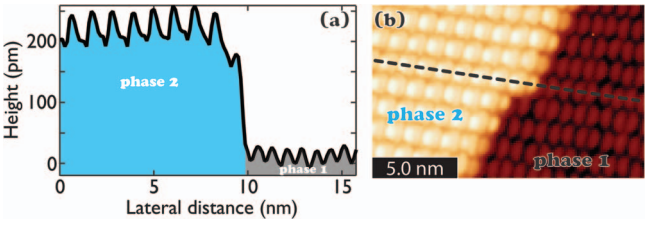

FIG. 2. (a) Cross-sectional plot taken along the line drawn in the STM image of (b). (b) STM image showing a boundary of phase 1 and phase 2 ($V_s = 1.74$ V, $I_t = 48$ pA).

The unit cell of phase 2, indicated as a white parallelogram in Fig. 1(e), has a length of 1.09 ± 0.06 nm and 1.42 ± 0.08 nm with an angle of 73° ± 3°, which corresponds to the molecular density of 1.48 ± 0.08 molecules/nm^2. We found that the distance between the tilted molecules is almost same as the length along [110] (1.055 nm) or [1$\bar{1}$0] (1.041 nm) of the monoclinic unit cell of crystalline picene.[25] The measured distance between the molecular rows, 1.36 nm, also coincides with the *c*-axis length (1.35 nm) of the picene crystal. We thus speculate that the (110) or (1$\bar{1}$0) layer of crystalline picene is formed on the substrate with the orientational relation of [110](110) picene // [110](111) Ag, except for the relation of the molecular positions between the neighboring rows, which is not exactly the same as that of the crystal.

The observed molecular stacking is in contrast with the case of pentacene on the same substrate.[24,26] In the case of pentacene the adsorbed molecules form a (011) plane, which is composed of tilted molecules only. The bulk-like pentacene layer is formed on a chemisorbed wetting molecular layer underneath, which is also different from the case of picene, where the bulk-like layer is formed directly on the substrate. The difference in structures arises from the different interaction between the molecules and substrate; pentacene exhibits chemical interaction with the Ag(111) substrate while picene does not, as will be discussed below.

C. Theoretical calculations on monolayer picene phases

In order to investigate the stability of the proposed models and elucidate the nature of the interaction between the molecules and substrate for the two phases, we performed first principles DFT calculations for the structures of phase 1 and phase 2. For the calculations the molecular lattice was slightly adjusted so that it is commensurate with the substrate lattice. The unit cell of phase 1 and 2 was fixed at $\begin{pmatrix} 6 & -6 \\ 5 & 5 \end{pmatrix}$ and $\begin{pmatrix} -5 & 1 \\ 4 & 4 \end{pmatrix}$ with respect to the Ag(111) unit cell, with four and two picene molecules adsorbed on one side of the Ag(111) slab in the unit cell, respectively.

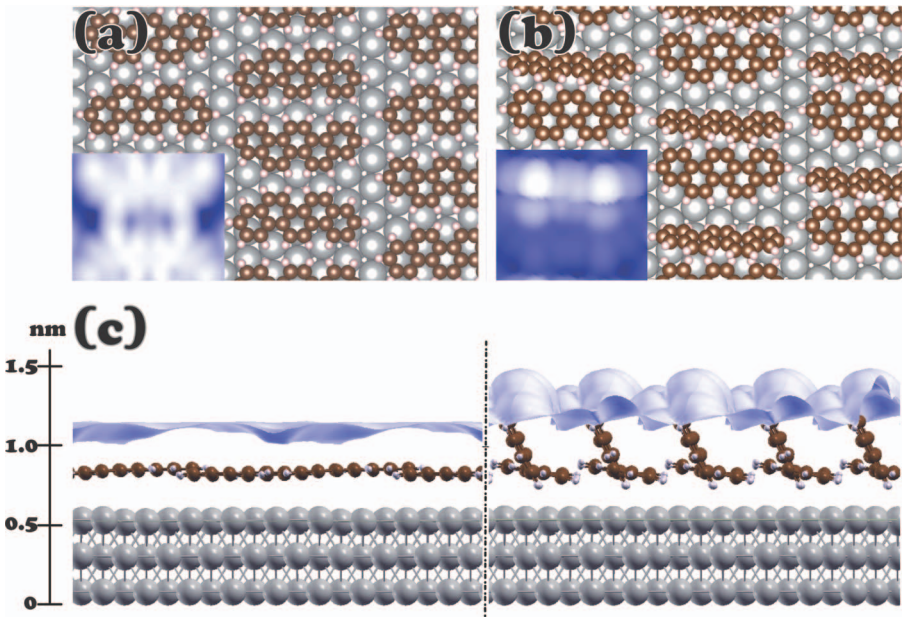

FIG. 3. (a) Structural model for phase 1 obtained by the DFT calculation. The inset shows a simulated STM image. (b) Structural model for phase 2 and its simulated STM image (inset). (c) Cross-sectional view of the structural models and the simulated images for phase 1 and phase 2.

The energetically stable structure after the structural relaxation for the two phases is shown in Figs. 3(a) and 3(b). The adsorption energy per molecule is −2.31 eV and −2.39 eV for phase 1 and phase 2, respectively. The larger adsorption energy of phase 2 is due to intermolecular interaction in the bulk-like structure. In phase 1, the molecule-substrate interaction dominates the adsorption energy and is maximized by the almost cofacial adsorption geometry. In phase 2, on the other hand, the molecules which have herringbone-like geometry, show significant vdW interaction amongst themselves while the molecule-substrate interaction could be smaller than in phase 1. Recent theoretical studies using accurate vdW density functionals indicate that binding energies of crystalline hydrocarbons such as anthracene and rubrene are larger than 1.0 eV per molecule, implying the significance of the non-covalent vdW interaction in the herringbone-like stacked thin film.[27–29] The vdW interaction between the neighboring picene molecules contribute to the stability of phase 2 over phase 1.

Simulated STM images for the two structures are also shown in the insets of Figs. 3(a) and 3(b), respectively. The bias voltage set for the simulation is 1.0 V for phase 1 and 1.35 V for phase 2 to cover the LDOS of the lowest unoccupied molecular orbital (LUMO) state of the respective phases, the same as the case of the experimental STM images shown in Figs. 1(d) and 1(e). Although the experimental STM images do not show fine intra-molecular structures that appear in the simulated ones, the overall shape and conformation of the molecules are consistent. These results support the structural models estimated from the experimental STM images. The distance between the C atoms of the molecule and Ag atoms of the substrate in phase 1 is 3.0–3.2 nm, almost equal to the sum of the vdW radii of the two elements, suggesting a vdW interaction between them.

We measured the height difference between the two simulated STM images in order to compare with the experimental STM results (Fig. 2(a)). The bias voltage of the cross-section of the LDOS contour mappings, shown in Fig. 3(c), was set at 1.80 V so that the LDOS covers both LUMO and LUMO+1 states, as is the case of the corresponding experimental image. The theoretical height difference is ∼0.3 nm, similar to but even larger than the experimental value, ∼0.22 nm. The theoretical small height difference also rules out the possibility that phase 2 is formed on either phase 1 or a wetting layer.

D. Tunneling spectroscopy

Tunneling spectra taken on different structures exhibit distinct differences (Fig. 4(a)). The spectrum taken on an isolated molecule (submonolayer) has a shallow gap of ∼3.0 eV around the Fermi level. In the gap, a step-like feature with an onset at +0.1 eV can be seen, and the shape is quite similar with that observed on bare Ag(111) substrates, whose bottom is located at −0.12 eV.[30] Characteristic to tunneling spectra of the Shockley surface states, the step-like feature has a sharp onset that corresponds to the bottom of the two-dimensional electronic states and a slow decay into the high energy side, which is due to the suppressed tunneling probability for electronic states with large surface-parallel wave number.[31] Similar step-like features have been observed on monolayer molecules on (111) surfaces of noble metals,[32–35] and attributed to the Shockley surface states of the substrate.[33–35] As seen from a comparison with the spectrum taken on bare Ag(111) surfaces, the onset energy is shifted to the high energy side. The shift can be explained by considering the origin of the Shockley states, as will be discussed below. We thus attribute the step-like feature observed on a single adsorbed molecule to the modified surface states of Ag(111).

The energy level of the surface states is determined by the confinement of the wave functions in the direction perpendicular to the surface. In the case of the clean Ag(111) surface, the wave function is confined between the projected band gap

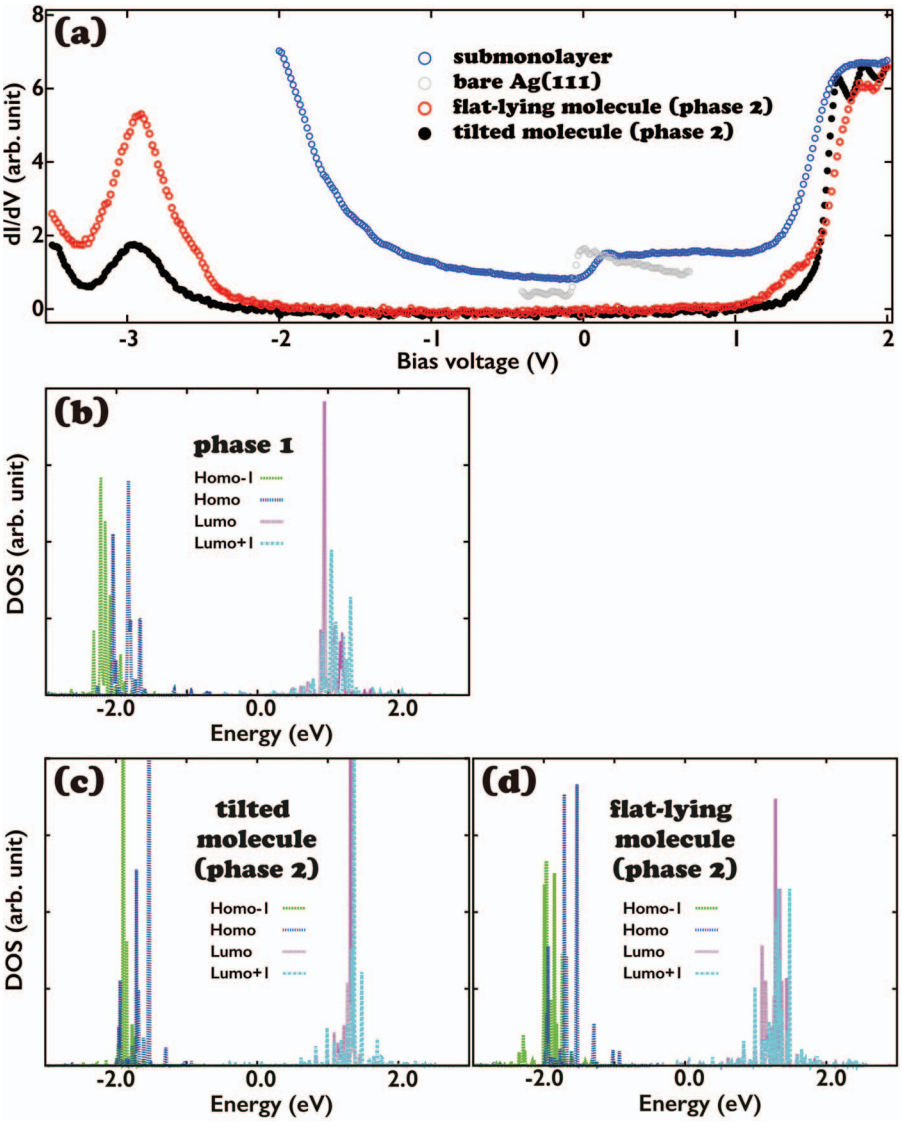

FIG. 4. (a) Tunneling spectra taken of submonolayer coverage picene deposited on a Ag(111) substrate (gray circle), as well as tilted and flat-lying molecules in the phase 2 structure of a picene thin film (black and red circles, respectively). They were taken after stabilizing the tip position with the tunneling condition of $V_s = -2.0$ V and $I_t = 200$ pA for the submonolayer spectra and $V_s = 2.0$ V and $I_t = 200$ pA for the phase 2 spectra. A spectrum taken on bare Ag(111) substrate (gray circles) is also shown as a reference ($V_s = -2.0$ V and $I_t = 1$ nA). (b) and (c) Projected LDOS of highest occupied molecular orbital (HOMO), HOMO-1, LUMO, and LUMO+1 on the molecules of phase 1 (b) and on the tilted and flat-lying molecules of phase 2 (c).

in the (111) direction of bulk Ag and the vacuum level whose height is related to the work function.[36–38] By the presence of the molecule, the confinement condition is modified by an extra phase in the wave function induced by an electrostatic potential of the molecule. Because of the additional phase in the wave function the energy level of the surface state is shifted from −0.12 eV to +0.1 eV. While the energy level is slightly modified by the adsorption of the molecule, the observation of the surface state itself indicates that the states originating from the 5*s*-orbital of the substrate do not significantly hybridize with the molecular orbitals.

In the submonolayer tunneling spectrum a steep increment around 1.4 eV presumably due to the LUMO state is observed while observation of other molecular states such as the HOMO was hampered by significant tunneling contribution from the metallic substrate through the adsorbed molecule.[34] Any peak structures which might be due to hybridized states, such as the one observed on pentacene adsorbed on Cu(111) substrate[23] are, however, not found in the tunneling spectra. It seems that no hybridization occurs between the adsorbates and the substrate in the present case.

Tunneling spectra taken on tilted and flat-lying molecules in phase 2, which is a bulk-like molecular monolayer, exhibit a strong gap ranging from −2.6 to 1.4 eV. The amount of the gap (4.0 eV) is larger than that measured on picene thin films (3.3 eV)[39] because of less dispersion in the direction perpendicular to the substrate. Our LDOS calculation for phase 2 (Fig. 4(c)) shows the gap of 2.5–2.8 eV depending on the measured sites. The smaller gap than the experiment has been reported in local density approximation (LDA) and generalized gradient approximation (GGA) of the DFT calculation; the theoretically estimated gap for crystalline picene (2.4 eV)[39] is also smaller than that of experiment (3.3 eV).

The spectrum taken on tilted (flat-lying) molecules shown in Fig. 4(a) exhibits peaks at −3.0, 1.7, and 1.9 eV (−3.0, −1.8, and −2.0 eV), although we found that the peak energy differences between the two molecules fluctuate by ∼0.15 eV probably due to variation in the local intermolecular configuration. While the energy levels of the HOMO state of the two molecules do not differ, the energy levels of the LUMO and LUMO+1 states taken on flat-lying molecules are in general higher than those of tilted molecules. When the intermolecular distance is small, the Pauli repulsion induces charge redistribution in the molecules and substrate, modifying the electrostatic potential of the relevant molecules and their electronic states.[11] The peak energies of LUMO and LUMO+1 states obtained by our first principles calculation shown in Fig. 4(c) are almost same between the tilted and flat-lying molecules. The same calculation performed with a unit cell smaller in size by 82%, however, showed higher LUMO and LUMO+1 states on flat-lying molecules than tilted ones by 0.2 eV. This indicates that local variation in the intermolecular distance modifies the local potential of the molecules and induces the peak energy differences between the two molecules.

The calculated spectra exhibit several peaks with small energy dispersion, as shown in Figs. 4(c) and 4(d). Both the experimental and theoretical tunneling spectra on phase 2 do not show any features in the gap, which indicates negligible hybridization between the orbitals of the adsorbed molecules and the electronic states of the substrate in the phase. Several very tiny peaks can be found in the theoretical results, but these peaks are not large enough to produce peak structures in tunneling spectra like the ones observed by Smerdon *et al.*[23] on pentacene/Cu(111) and Gonzalez-Lakunza *et al.*[33] According to the Mulliken population analysis the amount of charge transfer from the substrate to the LUMO and LUMO+1 states of the tilted and flat-lying molecules due to the gap states is only 0.02*e* and 0.04*e*, respectively, where *e* is the electron charge. It is not reasonable to claim chemisorption from such small amounts of charge transfer. Note that the tip-sample distance during our tunneling conductance measurements is similar to or even smaller than that of Gonzalez-Lakunza *et al.*,[33] who observed peaks due to hybridized states at the TCNQ/Au(111) interface, judged from a comparison of the two stabilization conditions. We thus do not think our tip-sample distance was too far to detect hybridized states. A theoretical tunneling spectrum of phase 1 (Fig. 4(b)) does not show peaks in the gap either. All these results lead us to conclude that the interaction between the molecule and the substrate is dominated by the vdW interaction and that the contribution of the chemical interaction is negligibly small.

The weak interaction and the vdW binding nature of the molecule to the substrate are quite different from the case of the sister molecule, pentacene. The straight 5-benzene-ring molecule is known to chemisorb on Cu(111)[40–42] and Ag(111)[24,26] surfaces; the hybridized states between the molecular orbitals and substrate states and their energy dispersions have been observed experimentally by angle-resolved photoemission spectroscopy,[41] and reproduced theoretically by first principles calculations.[42] We attribute the difference in the bonding nature between the two 5-benzene-ring molecules to the difference in their band gap; picene has wider band gap than pentacene, and therefore the energy levels of the molecular states of picene are far from the Fermi level. Large energy differences between the molecular orbitals and the relevant electronic states of the substrate suppress hybridization between them. As a consequence of the different bonding nature, the growth modes of the thin films of the two molecules are quite different; Thayer *et al.*[43] reported that pentacene molecules form a flat-lying layer on strongly interacting metallic substrates, while on weakly-bound semi-metal Bi substrates bulk-like structures are formed directly on the surface. The bulk-like structure in phase 2 directly bound to the substrate is attributed to the weak physisorbed interaction between the picene molecules and the Ag(111) substrate.

In order to investigate details of the observed electronic states on the adsorbed molecules, we performed two-dimensional tunneling spectroscopy. Figure 5 shows tunneling conductance (*dI/dV*) mappings, which correspond to the spatial distribution of LDOS at each energy level. In the topographic image (Fig. 5(b)), a tilted molecule is enclosed with a dashed oval and its center is marked with a red circle. The *dI/dV* mappings show a node at the center of the tilted molecule at 1.76 eV (Fig. 5(d)) whereas no nodes are observed at 1.95 eV (Fig. 5(e)). Since the LUMO (LUMO+1) states of the molecule have (do not have) a node at the center of the long molecular axis,[39] the observed node features indicate that the tilted molecule in phase 2 have DOS close to a single picene molecule. This is in contrast with the case of crystalline picene, where LUMO and LUMO+1 states of the constituent molecules are coupled to show similar DOS distributions at the two energy levels in the conduction band.[39] This indicates that, although phase 2 has a structure similar to that of bulk, its electronic states of LUMO and LUMO+1 are not; one monolayer is not enough to have bulk band states.

E. Monolayer structure with standing molecules

We also observed a monolayer structure in which all molecules are standing. As shown in the STM image of

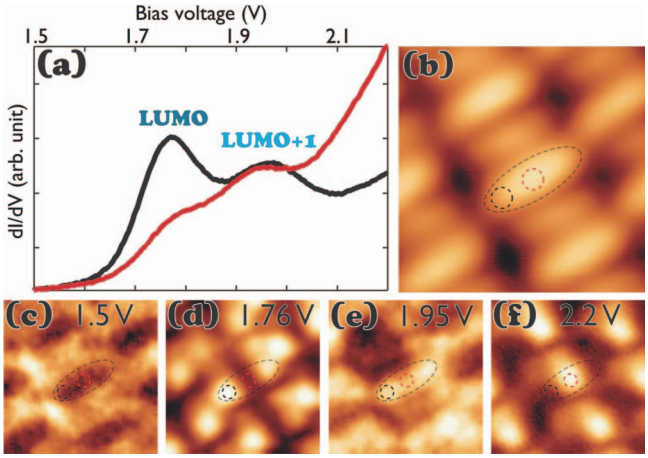

FIG. 5. (a) Tunneling spectra taken at the center (red) and edge (black) of a tilted molecule in phase 2. (b) STM image (V_s = 2.2 V, I_t = 200 pA), and (c)–(f) tunneling conductance (*dI/dV*) mappings at 1.5 V, 1.76 V, 1.95 V, and 2.2 V, respectively, taken on phase 2. The stabilization condition for the spectroscopy is V_s = 2.2 V and I_t = 200 pA.

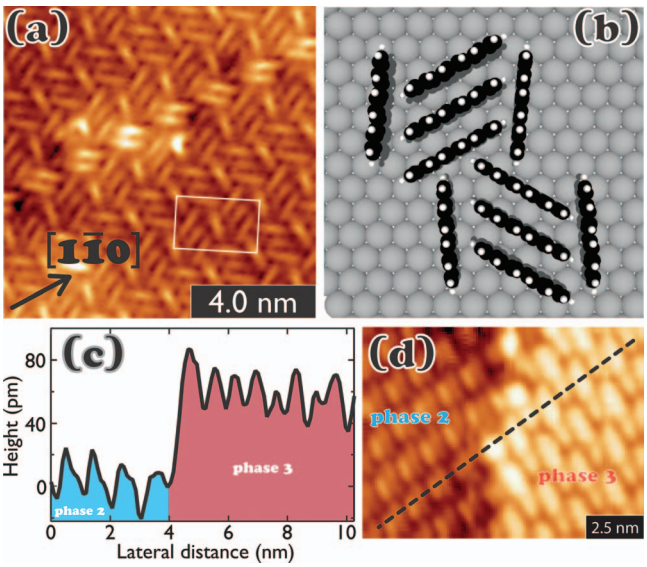

FIG. 6. (a) STM image of phase 3 of picene molecules adsorbed on Ag(111) substrate ($V_s = 1.0$ V and $I_t = 360$ pA). (b) Schematic model of the adsorbed molecules for phase 3. (c) Cross-sectional plot taken along the line in the STM image of (d). (d) STM image showing a boundary of phase 2 and phase 3 ($V_s = 1.0$ V, $I_t = 360$ pA).

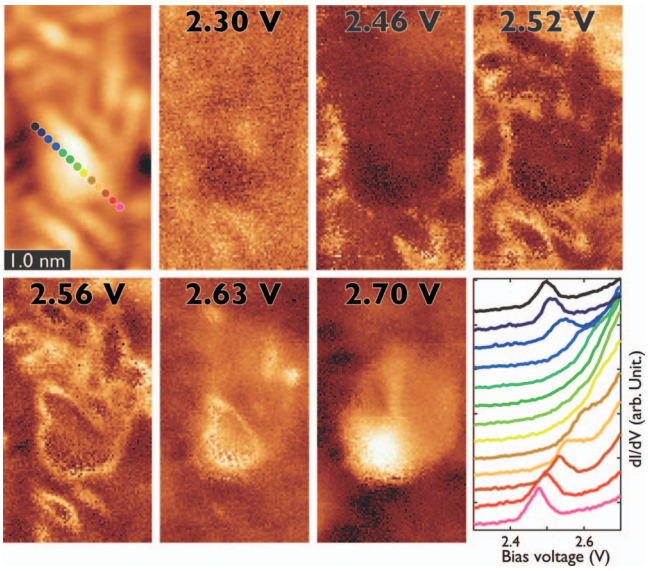

FIG. 7. STM image ($V_s = 2.7$ V, $I_t = 293$ pA), *dI/dV* mappings at 2.3 V, 2.46 V, 2.52 V, 2.56 V, 2.63 V, and 2.70 V, and tunneling spectra taken at the positions marked in the STM image with the corresponding colors, on a K-deposited phase 3 structure. The stabilization condition is $V_s = 2.7$ V and $I_t = 293$ pA.

Fig. 6(a), all molecules are observed as a narrow bright protrusion. Since the length of the protrusions corresponds to that of the long axis of the molecule, we presume that the molecules are standing with their long axis parallel to the substrate. In this configuration aromatic rings of the neighboring molecules face each other, and, therefore, attractive intermolecular interaction due to π stacking is expected. The structure, which we call phase 3, has a rectangular unit cell, shown as a white box in Fig. 6(a), with glide symmetry (*p2gg*) whose length is given by 1.56 ± 0.1 nm and 2.72 ± 0.16 nm. The short axis of the unit cell is along the [1$\bar{1}$0] direction of the substrate. As the unit cell has 8 molecules, the molecular density is 1.89 molecules/nm^2.

Since the height difference between phase 3 and phase 2 is just 0.05 nm (Fig. 6(c)), a monolayer of phase 3 also seems directly formed on the substrate without any ordered or disordered layers underneath. Note that because of a blunt probe tip individual molecules in phase 3 are not resolved in the image. A possible molecular arrangement is schematically presented in Fig. 6(b). Since all molecules are standing with π stacking, electronic states delocalized in the layer are expected.

F. Potassium adsorption on a monolayer picene structure

In order to investigate the role of the alkali metals on the electronic delocalization, we deposited K on the phase 3 structure and measured tunneling spectra as shown in Fig. 7. The amount of the deposited K is 1.7 atoms per molecule. The tunneling spectra show a peak around +2.5 V, and the peak position gradually shifts to the higher voltage as the tip moves toward an unknown protrusion shown in the topographic image. Tunneling conductance (*dI/dV*) mappings clearly demonstrate the gradual shift; contour-like bright rings that are strongly deformed by the local molecular configuration are found in the mappings, and the rings shrink toward the protrusion with the bias voltage. The observed gradual shift and its contour-like ring features are explained by the spatial variation in electrostatic potential.[44,45] Since the potential goes up towards the protrusion, there should be a negative charge at the protrusion; around the negative charge the potential that electrons feel is raised and the whole electronic structure including the 2.5 eV state shifts to higher energy in a rigid manner. The energy level of the state thus follows the spatial distribution of the potential, which creates ring-like potential contours around its maxima and minima.

Similar ring-like structures in *dI/dV* mappings can be formed by the tip-induced charging of dopants.[46,47] In the case of the tip-induced charging, however, rings are rather circular and not severely modified by the local structure. In fact, if the ring-like structures are due to the charging, as is the case of Refs. 46 and 47, they do not behave like a contour; when two rings meet, the two rings just overlap each other. In the case of the potential, however, the two rings are merged to form a cocoon-like shape. As the rings we observed do not overlap, we presume it is due to the potential variation.

According to the Poisson equation, the potential variation requires charged carriers, as in the case of band bending in semiconducting materials. In semiconductors, the spatial variation of the potential is characterized by the Debye length, which is inversely proportional to the square-root of the carrier density. Since our experiments show potential variation in nano-meter scale, we conclude the presence of a significant amount of mobile carriers in the molecular thin film, indicating the existence of delocalized states. The observed nano-scale potential shift is a clear indication of 2D delocalized electronic states in the molecular thin film, which is induced by the π-stacking formed in the molecular structure of phase 3.

IV. SUMMARY

Using STM/STS and DFT calculations, we have investigated pristine and K-deposited thin films of picene molecules formed *in situ* on Ag(111) substrate. Through the observation of the molecular structures and their electronic properties, we found that the growth of picene and its electronic states are rather different from pentacene because of the weak vdW interaction of the molecule with the substrate. The weak interaction is due to the large band gap of the molecule and negligible hybridization between the molecular orbitals and the substrate electronic states. Our results provide nanoscale insight on the thin film formation of the molecule and its electronic states, which shows promise as a conductive channel of molecular field effect transistors and a base material of organic superconductors that exhibit high critical temperatures.

ACKNOWLEDGMENTS

Discussion with Howon Kim is greatly appreciated. S.Y. acknowledges Ikutaro Hamada and Yoshitada Morikawa for helpful comments and advice on the calculated results. The authors also appreciate Jack Hellerstedt for critical reading. G.H. appreciates support from Invitation Fellowship Programs for Research in Japan, Japan Society for the Promotion of Science. This work is partially funded by Grants-in-Aid for Scientific Research, Japan Society for the Promotion of Science (Grant Nos. 21360018, 23840008, 25286055, 26110507, and 26120508). The numerical calculations were carried out at the computer center of Institute for Solid State Physics, The University of Tokyo.

[1]D. J. Gundlach, Y. Y. Lin, T. N. Jackson, and D. G. Schlom, IEEE Electron Device Lett. **18**, 87 (1997).
[2]C. D. Dimitrakopoulos and P. R. L. Malenfant, Adv. Mater. **14**, 99 (2002).
[3]T. W. Kelley, P. F. Baude, C. Gerlach, D. E. Ender, D. Muyres, M. A. Haase, D. E. Vogel, and S. D. Theiss, Chem. Mater. **16**, 4413 (2004).
[4]S. Yoo, B. Domerq, and B. Kippelen, Appl. Phys. Lett. **85**, 5427 (2004).
[5]A. K. Pandey and J.-M. Nunzi, Appl. Phys. Lett. **89**, 213506 (2006).
[6]H. Okamoto, N. Kawasaki, Y. Kaji, Y. Kubozono, A. Fujiwara, and M. Yamaji, J. Am. Chem. Soc. **130**, 10470 (2008).
[7]R. Mitsuhashi, Y. Suzuki, Y. Yamanari, H. Mitamura, T. Kambe, N. Ikeda, H. Okamoto, A. Fujiwara, M. Yamaji, N. Kawasaki, Y. Maniwa, and Y. Kubozono, Nature (London) **464**, 76 (2010).
[8]X. F. Wang, R. H. Liu, Z. Gui, Y. L. Xie, Y. J. Yan, J. J. Ying, X. G. Luo, and X. H. Chen, Nat. Commun. **2**, 507 (2011).
[9]M. Xue, T. Cao, D. Wang, Y. Wu, H. Yang, X. Dong, J. He, F. Li, and G. F. Chen, Sci. Rep. **2**, 389 (2012).
[10]Y. Shen, A. R. Hosseini, M. H. Wong, and G. G. Malliaras, ChemPhysChem. **5**, 16 (2004).
[11]H. Ishii, K. Sugiyama, E. Ito, and K. Seki, Adv. Mater. **11**, 605 (1999).
[12]N. Ashcroft and N. Mermin, *Solid State Physics* (Saunders College, Philadelphia, 1976).
[13]Y. Morikawa, H. Ishii, and K. Seki, Phys. Rev. B **69**, 041403(R) (2004).
[14]D. Vanderbilt, Phys. Rev. B **41**, 7892 (1990).
[15]N. Troullier and J. L. Martins, Phys. Rev. B **43**, 1993 (1991).
[16]M. Methfessel and A. T. Paxton, Phys. Rev. B **40**, 3616 (1989).
[17]J. P. Perdew, K. Burke, and M. Ernzerhof, Phys. Rev. Lett. **77**, 3865 (1996).
[18]S. Grimme, J. Comput. Chem. **27**, 1787 (2006).
[19]J. Tersoff and D. R. Hamann, Phys. Rev. Lett. **50**, 1998 (1983).
[20]S. Lukas, G. Witte, and Ch. Wöll, Phys. Rev. Lett. **88**, 028301 (2001).
[21]I. Fernandez-Torrente, S. Monturet, K. J. Franke, J. Fraxedas, N. Lorente, and J. I. Pascual, Phys. Rev. Lett. **99**, 176103 (2007).
[22]A. Scarfato, S.-H. Chang, S. Kuck, J. Brede, G. Hoffmann, and R. Wiesendanger, Surf. Sci. **602**, 677 (2008).
[23]J. A. Smerdon, M. Bode, N. P. Guisinger, and J. R. Guest, Phys. Rev. B **84**, 165436 (2011).
[24]D. B. Dougherty, W. Jin, W. G. Cullen, J. E. Reutt-Robey, and S. W. Robey, J. Phys. Chem. C **112**, 20334 (2008).
[25]A. De, R. Ghosh, S. Roychowdhury, and P. Roychowdhury, Acta Crystallogr., Sect. C: Cryst. Struct. Commun. **41**, 907 (1985).
[26]D. Käfer and G. Witte, Chem. Phys. Lett. **442**, 376 (2007).
[27]A. Otero-de-la-Roza and E. R. Johnson, J. Chem. Phys. **137**, 054103 (2012).
[28]A. M. Reilly and A. Tkatchenko, J. Chem. Phys. **139**, 024705 (2013).
[29]I. Hamada, Phys. Rev. B **89**, 121103(R) (2014).
[30]S. D. Kevan and R. H. Gaylord, Phys. Rev. B **36**, 5809 (1987).
[31]J. Li, W.-D. Schneider, R. Berndt, O. R. Bryant, and S. Crampin, Phys. Rev. Lett. **81**, 4464 (1998).
[32]R. Temirov, S. Soubatch, A. Luican, and F. S. Tautz, Nature (London) **444**, 350 (2006).
[33]N. Gonzalez-Lakunza, I. Fernández-Torrente, K. J. Franke, N. Lorente, A. Arnau, and J. I. Pascual, Phys. Rev. Lett. **100**, 156805 (2008).
[34]W.-H. Soe, C. Manzano, A. De Sarkar, N. Chandrasekhar, and C. Joachim, Phys. Rev. Lett. **102**, 176102 (2009).
[35]B. W. Heinrich, L. Limot, M. V. Rastei, C. Iacovita, J. P. Bucher, D. M. Djimbi, C. Massobrio, and M. Boero, Phys. Rev. Lett. **107**, 216801 (2011).
[36]N. V. Smith, Phys. Rev. B **32**, 3549 (1985).
[37]Th. Fauster, Appl. Phys. A **59**, 639 (1994).
[38]T. Suzuki, Y. Hasegawa, Z.-Q. Li, K. Ohno, Y. Kawazoe, and T. Sakurai, Phys. Rev. B **64**, 081403 (2001).
[39]T. Kosugi, T. Miyake, S. Ishibashi, R. Arita, and H. Aoki, J. Phys. Soc. Jpn. **78**, 113704 (2009).
[40]A. Ferretti, C. Baldacchini, A. Calzolari, R. D. Felice, A. Ruini, E. Molinari, and M. G. Betti, Phys. Rev. Lett. **99**, 046802 (2007).
[41]H. Yamane, D. Yoshimura, E. Kawabe, R. Sumii, K. Kanai, Y. Ouchi, N. Ueno, and K. Seki, Phys. Rev. B **76**, 165436 (2007).
[42]K. Toyoda, I. Hamada, S. Yanagisawa, and Y. Morikawa, Appl. Phys. Express **3**, 025701 (2010).
[43]G. E. Thayer, J. T. Sadowski, F. M. zu Heringdorf, T. Sakurai, and R. M. Tromp, Phys. Rev. Lett. **95**, 256106 (2005).
[44]M. Ono, Y. Nishigata, T. Nishio, T. Eguchi, and Y. Hasegawa, Phys. Rev. Lett. **96**, 016801 (2006).
[45]K. Hashimoto, C. Sohrmann, J. Wiebe, T. Inaoka, F. Meier, Y. Hirayama, R. A. Römer, R. Wiesendanger, and M. Morgenstern, Phys. Rev. Lett. **101**, 256802 (2008).
[46]N. A. Pradhan, N. Liu, C. Silien, and W. Ho, Phys. Rev. Lett. **94**, 076801 (2005).
[47]K. Teichmann, M. Wenderoth, S. Loth, R. G. Ulbrich, J. K. Garleff, A. P. Wijnheijmer, and P. M. Koenraad, Phys. Rev. Lett. **101**, 076103 (2008).